Fault Mitigation for Autonomous Vehicles with Reduced Front Steering Capability

Lateefa Shibah Tusuubira and Wen-Chiao Lin
Department of Electrical and Computer Engineering
Kettering University
Flint, MI 48504
Email: {tusu6353,wlin}@kettering.edu

Jun Chen
Department of Electrical and Computer Engineering
Oakland University
Rochester, MI 48309
Email: junchen@oakland.edu

***Abstract*—Recently developed autonomous vehicles utilize electric power steering (EPS) systems as their main front steering actuator. However, electrical connection from the vehicle battery to the EPS system may corrode due to water intrusion or humidity, increasing electrical resistance in the EPS power circuit. Under this situation, if the EPS is required to provide significant amount of power to steer the vehicle, loss of steering may occur due to decreased voltage seen at the EPS controller or reduced power transfer capability in the circuit. As drivers (or passengers) are not required to take over control of the vehicle in case of vehicle malfunction, loss of steering causes significant safety hazard for the vehicle and other users of the road. In this paper, fault mitigation strategies are proposed to reduce the EPS effort in case of increased power circuit resistance. Specifically, strategies based on model predictive control are developed that coordinate vehicle lateral motion actuation such as EPS, steering differential torque, and rear steering under increased EPS power circuit resistance. Simulation results show that voltage drop at the EPS controller due to the increased resistance can be reduced while the vehicle can still satisfactorily complete desired lane change maneuvers.**

I. Introduction

A. Motivation

The operation of a typical autonomous vehicle (AV) is described as follows. Sensors (e.g., IMU, cameras, radars, lidars) collect information as input to a perception system. Subsequently, based on the perception results and user defined mission inputs, a path/trajectory planning module will generate control objectives (e.g., desired path or trajectories) for feedback algorithms to control the vehicle via the actuators. In AVs (e.g., SAE automation levels 4 and 5 [1]), the driver is not required to monitor vehicle performance and take over driving of the vehicle in case of emergencies. In some designs, the driver may not even have the mechanism to steer, brake, and control the vehicle [2]. As such, for AVs to operate properly, the various vehicle components have to perform as expected. Unfortunately, sensors and actuators may experience faults/failures due to natural degradation (e.g., friction build up in the steering system [3], [4]) or malfunction (e.g., power wire loose or disconnection in power circuits [5], [6]). When faults/failures occur in chassis actuators critical to vehicle motions, there is no human backup. To ensure safety and avoid hazards, it is critical for the vehicle to still achieve acceptable performance without driver intervention.

B. Fault considered

In this paper, we focus on faults/failures of the front steering system of an AV, namely, the electric power steering (EPS) system, which is critical to the vehicle's lateral motions. In particular, an EPS system replaces traditional hydraulic power steering systems and steers the vehicle through an electric motor. Depending on vehicle designs, the EPS system may be mounted on a steering column or directly mounted on the steering rack/pinion of the vehicle. Fig. 1 illustrates the typical power connection of an EPS system. Specifically, the

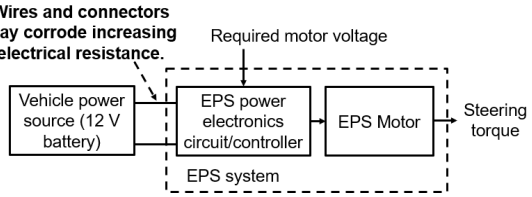

Fig. 1. Concept of EPS systems.

vehicle power source (i.e, the 12 volt battery) is connected to the power electronics circuit/controller (PEC) of the EPS system, forming a power circuit. Based on desired maneuver, a required motor voltage command is sent to the PEC, which generates the required voltage to drive the steering motor. The steering motor in turn

provides torque that steers the vehicle. However, the power connectors and wires that connect the EPS system to the vehicle power source may corrode (e.g., due to water intrusion or humidity), resulting in increased resistance in the EPS power circuit. When the EPS is required to provide a significant amount of power to steer the vehicle, the increased resistance may cause several issues such as decreased voltage seen by the EPS PEC or reduced electrical power transfer capability, which lead to loss of steering capability. Such issues have occurred in conventional (non-automated) vehicles [7], causing additional costs to vehicle manufacturers. In this paper, we propose fault mitigation algorithms that reduce the EPS effort but can still maintain satisfactory lateral control of the vehicle despite occurrences of the increased resistance. In particular, most AVs are built on electric vehicle platforms, which have independent traction motors. By adjusting the traction torque on the left and right side of the vehicle, differential steering torque can be generated for enhanced vehicle stability control [8]. Moreover, some recent electric vehicle are equipped with rear steering capabilities [9]. The differential torque and rear steer capabilities provide redundant lateral motion actuation that help steer the vehicle and reduce the required efforts from the EPS system. We utilize the recently pervasive model predictive control (MPC) methodology to coordinate these motion actuators, (i.e., EPS, differential torque, and rear steering) so that the vehicle can track a desired trajectory despite increase in EPS power circuit resistance.

C. Review of relevant literature

The work in this paper falls in the broad category of fault diagnosis, prognosis, and mitigation of vehicle safety critical components. While data-driven methods have been developed (see, e.g., [10], [11]), this work focuses mostly on model-based methods. Recent efforts focusing on components such as steering systems, brake system, and tires are documented in, e.g., [3]–[6], [12]–[18]. In particular, references [3]–[6] focus on faults/failures occurring in the EPS system. Reference [3] monitor the health of the EPS motor by utilizing online recursive estimation methods to estimate motor parameters. In addition, increase in the EPS friction is detected by monitoring the deviation of the self-aligning torque (SAT) estimated from two independent methods. Moreover, a fault signature table is constructed based on various health indicators to provide integrated EPS system diagnosis and fault isolation. Reference [4] provides refinement of the EPS friction detection algorithm and validation of it on a production vehicle. The work in [5] develops algorithms that provide prognostic solutions to EPS power connector faults (e.g., power connector loose and high resistance), which are the main source of intermittent failures in EPS systems. Specifically, power connector loose faults are addressed using a canary-based approach, while power connector high resistance faults are detected by an algorithm that uses power conservation arguments. This work is extended in [6], where fault mitigation algorithms are developed to avoid sudden loss of steering assist in conventional vehicles (i.e., non-automated) caused by high resistance in the EPS power circuit or a weak battery. Specifically, an "anti-loss-of-assist" strategy is developed there by gradually reducing steering assist when the resistance in the EPS power circuit increases. Brake system faults/failures are considered in [12]–[14]. In particular, [12] studies how brake rotor thickness variation (RTV) affects braking characteristics and proposes a failure prediction methodology that leverages time and frequency domain analysis to create health indicators (HIs) that assess rotor health and detect thickness variations of 36 microns or larger. The work in [13] builds on [12] and proposed a vibration-based fault detection and isolation algorithm that effectively detects and isolates RTV faults by analyzing vehicle signals before and during braking. Reference [14] encapsulates [12], [13] and proposes a classification model that distinguishes between healthy and faulty rotors by fusing the HIs to estimate the rotor state-of-health and isolate the most degraded rotor at the wheel or axle level and detect RTV levels of 20 microns or larger. Tire blowouts have also been investigated for ground vehicles in [15]–[18]. In particular, [15], [16] investigated the affects of tire blowout events on vehicle dynamics considering various vehicle chassis setups, while [17] developed shared control strategies upon tire blowouts for conventionally driven vehicles where the driver is still in control of the vehicle. Specifically, various metrics regarding the vehicle dynamic behavior is calculated to assist the driver in stabilizing the vehicle. The work in [18] further develop algorithms to automatically control an autonomously driving ground vehicle upon tire blowout.

This paper extends [6], where increased resistance in the power circuit of an EPS system is considered. A key assumption in [6] is that a driver is operating the vehicle and can provide enough steering torque to complete the steering maneuver in case of reduced steering assist. Hence, the work in [6] can only be used for conventional (non-automated) vehicles or vehicles of SAE automation levels 2 and 3 [1]. Here, we consider AVs (SAE automation levels 4 and 5 [1]), where the vehicle is driven autonomously with no one to make up for the

reduced steering torque. Without a proper control design, the vehicle would have to stop under severe EPS power circuit faults and, consequently, cause inconvenience for the driver and hazards for other users of the road. As mentioned above, redundant lateral motion actuation, such as differential torque and rear steering, afforded by recent electric vehicle platforms will be capitalized. An MPC algorithm is proposed to coordinate these actuation to complete a steering maneuver in case of increased resistance in the EPS power circuit. Other research on utilizing redundant vehicle motion actuation include [8], [19], [20]. In particular, [8] proposes a hierarchical control strategy for path tracking and energy-saving torque distribution in a six-wheel independent drive unmanned ground vehicle using differential steering to address actuator faults, vehicle stability, and energy efficiency. Reference [19] develops an overactuated autonomous ground vehicle aimed at enhancing safety and energy efficiency, while [20] proposes a fault-tolerant path tracking controller for a electric unmanned vehicle to maintain steering functionality in the event of complete steering failure by utilizing differential steering. The paper [21] gives a thorough survey of research conducted on fault tolerance designs of vehicle motion actuators. Finally, we mention [22] provides an introduction to MPC, while [23] documents recent developments and applications.

D. Main contributions and organization of paper

The main contributions of this paper include:

- Redundant lateral motion actuation available in modern vehicle platforms is utilized to extend technology developed for avoiding loss of steering due to EPS power circuit faults in conventional (non-automated) vehicles to AVs.
- MPC algorithms are applied to coordinate redundant lateral motion actuation for mitigating power circuit faults in EPS systems.

The rest of the paper is organized as follows. Section II describes steering issues caused by increased EPS power circuit resistance and outlines the proposed solution, while a simulation capability to develop, implement, and verify the solution is presented in Section III. Section IV details the proposed solution, and simulation results are given in Section V. Finally, conclusions and future work are described in Section VI.

II. Issues Addressed

Fig. 2 illustrates the EPS system along with its power circuit. In particular, V_B indicates the vehicle power source voltage (the 12 volt battery), I_C is the current from the vehicle power source to the EPS system, V_C is the voltage seen at the EPS PEC, V_M is the motor voltage (output of the EPS PEC), I_M is the motor current, R_M is the motor resistance, L_M is the motor inductance, θ is the motor angular position (with $\dot{\theta} = \omega$), and τ_m is the motor torque that steers the vehicle. The resistance in the EPS power circuit is modeled by R_C. Larger values of R_C indicate worse corrosion in the EPS power circuit. The increased resistance R_C causes two main

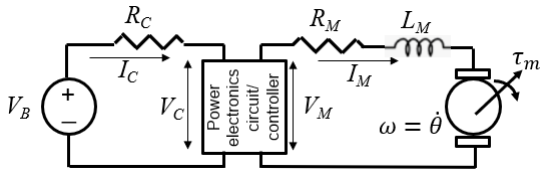

Fig. 2. EPS system with power circuit.

issues in the steering system: (1) large voltage drop at the EPS PEC, and (2) reduced maximum power transfer capability. These two issues may cause intermittent loss of steering as explained below. Assuming, when actively steering, the current in the EPS power circuit is I_C. With the increased resistance, voltage at the EPS PEC (V_C) is

$$V_C = V_B - I_C R_C. \tag{1}$$

As such, the larger R_C, the lower the voltage V_C is seen at the EPS PEC. Some EPS system designs have voltage thresholds V_{TH} so that when $V_C < V_{TH}$, the EPS system will automatically reset, causing instant loss of steering. Moreover, from the power circuit perspective, the power transferred from the vehicle power source to the EPS system can be described as $V_C I_C = -R_C(I_C - \frac{V_B}{2R_C})^2 + \frac{V_B^2}{4R_C}$, which reaches a maximum value at $\frac{V_B^2}{4R_C}$. Apparently, the larger R_C, the lower the maximum power that can be transferred to the EPS system. When the vehicle requires large amount of power for steering, the power circuit may not be able to transfer the required power, also causing loss of steering. To address these issues, we propose algorithms that reduce the required EPS effort but can still maintain satisfactory vehicle lateral movements. In particular, we capitalize on actuators in modern electric vehicle platforms that provide redundancy in generating vehicle lateral motion. Specifically, as explained in Section I-B, many modern electrical vehicles are equipped with traction motors which are independently driven, and as the power circuit resistance increases, differential torque can be generated to create additional yaw motion that assist steering, and, consequently, reduce EPS system efforts to avoid potential loss of steering. Similarly, some modern vehicles are equipped with rear steer capabilities, which can be

also used when the power circuit resistance increases. An MPC algorithm is used to coordinate these actuators so that reference trajectories can be followed satisfactorily.

III. Modeling

In order to develop and evaluate the proposed solution, a simulation capability is implemented in MATLAB/SIMULINK. A conceptual diagram is shown in Fig. 3. Specifically, a controller takes as inputs a desired

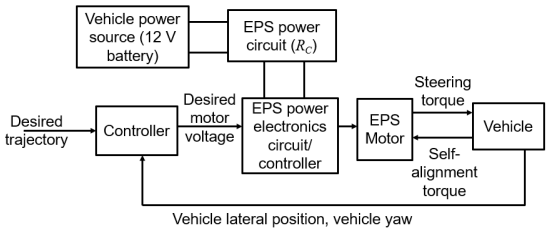

Fig. 3. Conceptual diagram of simulation capability.

reference trajectory as well as the actual vehicle position and yaw, and calculates the desired motor voltage as input the PEC of the EPS system. Consistent with the descriptions above, the PEC is connected to the vehicle 12 volt battery source via a power circuit, which may experience increased resistance, modeled by R_C. The PEC consequently steps up or steps down voltage from the power circuit so that the motor voltage matches the required motor voltage. The motor then generates the required torque to steer the vehicle, overcoming friction and the vehicle self-alignment torque (SAT). We discuss the baseline models for these components in the rest of this section, while modifications of them for the proposed solution are explained in the next section.

A. Vehicle model

We focus on lateral maneuvers, i.e., lane changes, of the vehicle, and, consequently, a lateral dynamics model is used. The bicycle model (see, e.g., [24]–[26]) below is used to simplify the vehicle dynamics by assuming the front and rear wheels are represented by single wheels:

$$\begin{bmatrix} \dot{v} \\ \dot{r} \end{bmatrix} = \begin{bmatrix} -\left(\frac{C_{\alpha f}+C_{\alpha r}}{mu_0}\right) & -\left(\frac{aC_{\alpha f}-bC_{\alpha r}}{mu_0^2}\right)-1 \\ -\left(\frac{aC_{\alpha f}-bC_{\alpha r}}{I_z u_0}\right) & -\left(\frac{a^2C_{\alpha f}+b^2C_{\alpha r}}{I_z u_0}\right) \end{bmatrix} \begin{bmatrix} v \\ r \end{bmatrix} + \begin{bmatrix} \frac{C_{\alpha f}}{m} \\ \frac{aC_{\alpha f}}{I_z} \end{bmatrix} \delta_f, \quad (2)$$

where v is the lateral velocity, r is the yaw rate of the vehicle, u_0 is the forward speed, $C_{\alpha f}$ is the cornering stiffness of the front tires, $C_{\alpha r}$ is the cornering stiffness of the rear tires, m is the mass of the vehicle, I_z is the moment of inertia of the vehicle, a is distance from center of gravity to the front axle, b is distance from center of gravity to the rear axle, and δ_f is the front road wheel angle.

B. Steering system

We assume the EPS system is column-type, in which the motor is positioned along the steering column and connected to the steering shaft through spur gears, delivering torque to the shaft [3]. The motor torque is applied to the steering shaft through the reduction gear, and the product of the motor torque and the gear ratio results in steering torque on the shaft. The motor torque rotates the steering column against the SAT from the tires (through the steering rack and pinion mechanism) and the friction (e.g., damping) in the system. Referring to variables in Fig. 2, equations describing the EPS motor are:

$$L_M \frac{dI_M}{dt} + R_M I_M = V_M - K_e \omega, \quad (3)$$

$$\tau_m = K_t I_M, \quad (4)$$

where K_t and K_e are the torque and back EMF constants, respectively. It is assumed that $K_t = K_e$. The motion of the steering system is described as a whole rigid body with the motor and steering column dynamics given as $J_{eq}\ddot{\theta} + B_{eq}\dot{\theta} + K_{eq}\theta = \tau_m - \tau_{SAT,m}$, where J_{eq}, B_{eq}, and K_{eq} are the steering inertia, damping coefficient, and stiffness, respectively, seen from the motor side of the dynamics. Moreover, $\tau_{SAT,m}$ is the steering SAT also seen at the motor side. The SAT from the tire and road interaction is calculated as $\tau_{SAT} = \alpha C_{\alpha f} l_p$, where α is the front wheel slip angle and l_p is the pneumatic trail. This torque is seen as $\tau_{SAT,m} = \tau_{SAT}/(nG_r)$ on the motor, where G_r is the ratio from the steering column angle to the road wheel angle, and n is the gear ratio from the motor angular position to the steering column angular position. Note the relation between the motor position θ and front road wheel angle δ_f is $\theta = nG_r\delta_f$.

C. Power electronics circuit

We assume that the PEC is a buck-boost converter that is capable of handling varying input supply voltages V_C [27]. The converter will step up or step down V_C so that V_M matches the desired motor voltage command. As these converters typically have high chopping frequencies, we assume the converter is able to directly output the desired motor voltage command. Hence, the PEC block is modeled as an identity function from the desired motor voltage to V_M. To calculate the voltage V_C seen by the PEC, we utilize the power conservation argument used in [5], [6]. In particular, assuming negligible power losses in the PEC, motor circuit, and mechanical system,

we have $V_C I_C = \omega \tau_m$ (i.e., electrial power input equals mechanical power output). Using the power circuit equation (1), we approximate $V_C = \frac{V_B - \sqrt{V_B^2 - 4R_C \omega \tau_m}}{2}$.

D. Control architectures

Controllers based on MPC are proposed for this work. Specifically, MPC is a feedback control strategy that uses a mathematical model of a system to predict its future behavior over a defined prediction horizon. At each sampling time, using current state measurements and control inputs, the controller calculates the optimal control actions to ensure the system's output closely follows a reference trajectory while respecting system constraints. A cost associated with these actions are calculated based on penalties in magnitudes of the input and errors between the desired and predicted behaviors. For the application here, the vehicle is to follow a desired lane change trajectory, which is generated using waypoints for the lateral position (y) and yaw angle (ψ), ensuring that the vehicle transitions from its initial position ($y = 0$) to the target lane position ($y = 3.7$) both with $\psi = 0$. For the simulation capability, control action is the (desired) EPS motor voltage, and the cost function is $J = \sum_{k=1}^{p}[(w_y e_{y_k}^2) + (w_\psi e_{\psi_k}^2)] + \sum_{k=0}^{c}[(w_V V_k^2) + (w_{\Delta V} \Delta V_k^2)]$, where e_{yk} and $e_{\psi k}$ are the (predicted) position and yaw errors at time k, p is the prediction horizon, and c is the control horizon. Hence, the first summation is the weighted sum of squares of the predicted errors of the lateral position y and yaw ψ. Furthermore, the second summation is the weighted sum of squares of motor voltage and its increments.

IV. Fault Mitigation Strategies

In order to avoid sudden loss of steering explained in Section II, steering differential torque and rear steer will be utilized to reduce required steering effort from the EPS. We consider three strategies for fault mitigation:

(i) Use differential torque in addition to EPS: The MPC controller is modified to calculate both the required EPS motor voltage and differential torque to complete a required maneuver. Consequently, the cost used in the MPC is modified as $J = \sum_{k=1}^{p}[(w_y e_{y_k}^2) + (w_\psi e_{\psi_k}^2)] + \sum_{k=0}^{c}[(w_V V_k^2) + (w_{\Delta V} \Delta V_k^2) + (w_{DT} \tau_{DT}^2) + (w_{\Delta DT} \Delta \tau_{DT}^2)]$, where weighted sum of squares of the differential torque, τ_{DT}, and its increments are added to the cost. Moreover, to use the differential torque as a control actuation, the vehicle model is modified as:

$$\begin{bmatrix} \dot{v} \\ \dot{r} \end{bmatrix} = \begin{bmatrix} -\left(\frac{C_{\alpha f} + C_{\alpha r}}{m u_0}\right) & -\left(\frac{a C_{\alpha f} - b C_{\alpha r}}{m u_0^2}\right) - 1 \\ -\left(\frac{a C_{\alpha f} - b C_{\alpha r}}{I_z u_0}\right) & -\left(\frac{a^2 C_{\alpha f} + b^2 C_{\alpha r}}{I_z u_0}\right) \end{bmatrix} \times \begin{bmatrix} v \\ r \end{bmatrix} + \begin{bmatrix} \frac{C_{\alpha f}}{m} \\ \frac{a C_{\alpha f}}{I_z} \end{bmatrix} \delta_f + \begin{bmatrix} 0 \\ \frac{1}{I_z} \end{bmatrix} \tau_{TD}.$$

(ii) Use rear steer in addition to EPS: The MPC controller is modified to calculate both the required EPS motor voltage and rear steering angle to complete a required maneuver. Consequently, the cost used in the MPC is modified as $J = \sum_{k=1}^{p}[(w_y e_{y_k}^2) + (w_\psi e_{\psi_k}^2)] + \sum_{k=0}^{c}[(w_V V_k^2) + (w_{\Delta V} \Delta V_k^2) + (w_{\delta r} \delta_r^2) + (w_{\Delta \delta r} \Delta \delta_r^2)]$, where weighted sum of squares of the rear steering angle, δ_r, and its increments are added to the cost. Moreover, to use rear steer as a control actuation, the vehicle model is modified as:

$$\begin{bmatrix} \dot{v} \\ \dot{r} \end{bmatrix} = \begin{bmatrix} -\left(\frac{C_{\alpha f} + C_{\alpha r}}{m u_0}\right) & -\left(\frac{a C_{\alpha f} - b C_{\alpha r}}{m u_0^2}\right) - 1 \\ -\left(\frac{a C_{\alpha f} - b C_{\alpha r}}{I_z u_0}\right) & -\left(\frac{a^2 C_{\alpha f} + b^2 C_{\alpha r}}{I_z u_0}\right) \end{bmatrix} \times \begin{bmatrix} v \\ r \end{bmatrix} + \begin{bmatrix} \frac{C_{\alpha f}}{m} & \frac{C_{\alpha r}}{m} \\ \frac{a C_{\alpha f}}{I_z} & \frac{-b C_{\alpha r}}{I_z} \end{bmatrix} \begin{bmatrix} \delta_f \\ \delta_r \end{bmatrix}.$$

(iii) Use both differential torque and rear steer in addition to EPS: The MPC controller is modified to calculate required EPS motor voltage, differential torque, and rear steering angle to complete desired maneuvers. Hence, as in the above two strategies, the cost used in the MPC is similarly modified. Also as in the above two strategies, to use the differential torque as well as rear steer as control actuation, the vehicle model is similarly modified.

In the above strategies, we tacitly assumed that the subsystems creating the differential torque and rear steering angle react fast enough so that their dynamics are not considered in this study. A sensitivity analysis on these actuator delays will be conducted in future work.

V. Simulation Results

Simulations for the fault mitigation strategies in Section IV are conducted using the MATLAB/SIMULINK capability described in Section III. They are aimed at evaluating the effectiveness of the proposed strategies for mitigating loss of steering due to increased resistance, R_C, in the EPS power circuit. Each of the strategies is individually tested to determine its impact on completing the desired vehicle maneuver under the increased resistance. For comparison, it is assumed a vehicle is traveling at a constant velocity of $u_0 = 15$ m/s and

following the desired lane change maneuver described in Section III-D. This scenario represents a typical real world mid-speed highway driving condition. The lane change maneuver is associated with the vehicle's lateral dynamics, providing a robust scenario to evaluate the control strategies. Furthermore, parameters of the vehicle and motor models used in the simulations are indicated in Table I, and weights used in the MPC cost function for the mitigation strategies are given in Table II. Perfor-

TABLE I
PARAMETERS USED IN THE VEHICLE AND MOTOR MODELS.

Parameter	Value	Parameter	Value
m	1000 kg	R_M	3 mΩ
I_z	1400 kgm^2	L_M	1 mH
l	2.54 m	$K_t(K_e)$	0.5 Nm/A
a	1.14 m	B_{eq}	0.01 Nms/rad
b	1.4 m	l_p	0.03 m
$C_{\alpha f}$	1.37e5 N/rad	G_r	16.5
$C_{\alpha r}$	1.14e5 N/rad	n	20

TABLE II
PARAMETERS USED FOR MPC

Scenario	w_V	w_{DT}	$w_{\delta r}$	w_ψ	w_y	$w_{\Delta V}$	$w_{\Delta DT}$	$w_{\Delta \delta r}$
Baseline	0	–	–	1	1	0.1	–	–
Strategy (i)	1	0.5	–	1	5	0.1	0.1	–
Strategy (ii)	0.1	–	1	1	1	0.1	–	0.1
Strategy (iii)	0.5	1	1	1	2	0.1	0.1	0.1

mance observed for the simulations are: (α) Trajectory following: the deviations of the lateral position y from the reference trajectory; (β) Computed controller outputs for the strategy considered (e.g., motor voltage (V_M), differential torque (τ_{TD}), and rear steer angle (δ_r)); (γ) Voltage at the EPS PEC, V_C: as discussed in Section II, due to the increased resistance in the EPS power circuit, V_C will drop as the vehicle is actively steering, and if V_C drops under a certain threshold, loss of steering may occur. Through these observations, the simulation results highlight the efficacy of each fault mitigation strategy.

A. Baseline simulations

The baseline simulations evaluate the voltage V_C with increased R_C during a lane change maneuver with no mitigation strategies. In particular, we consider R_C = 60, 100, 150, and 200 mΩ. Fig. 4 shows the resulting lane change maneuver, motor voltage (V_M), and values of V_C for the various R_C considered. The following observations are made:

(a) Trajectory following: The MPC controller is able to calculate V_M required for the lane change. The lateral position y follows the reference trajectory with reasonable error. The resulting trajectories are the same for the considered values of R_C since we assumed (in Section III-C) that the EPS PEC are converters with high chopping frequencies.

(b) Voltage, V_C, at the EPS PEC: While the trajectory is followed accurately, the results of the simulation show a significant issue with V_C. For large values of R_C, the values of V_C experiences significant drops, increasing the possibility of loss of steering.

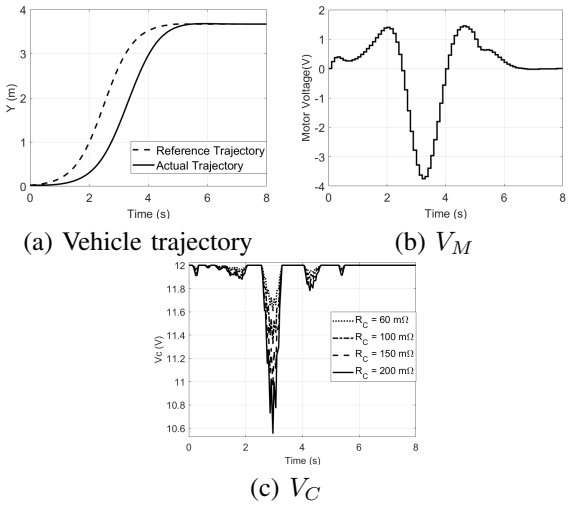

(a) Vehicle trajectory (b) V_M

(c) V_C

Fig. 4. Simulation results for the baseline simulations.

Results from the base simulations show the limitations of relying solely on front steering for an EPS system with increased R_C. While the MPC allow for trajectory following, the inability of the EPS power circuit to maintain sufficiently high V_C poses a significant risk of losing steering assist, especially in dynamic maneuvers.

B. Mitigation strategy (i) simulation

The differential torque, τ_{DT}, is generated by adjusting the traction torque between the left and right wheels, provides additional yaw control, reducing the reliance on the EPS system to generate steering moments. Fig. 5 shows the resulting lane change maneuver, motor voltage (V_M), calculated differential torque, and values of V_C for R_C = 200 mΩ. The following observations are made:

(a) Trajectory following: Similar to the baseline simulation, the MPC controller ensures that the vehicle closely tracks the reference trajectory. This highlights effectiveness of MPC in managing complex dynamics, coordinating steering redundancies.

(b) Improved EPS voltage stability: Introduction of τ_{TD} significantly reduces the effort of EPS motor. Consequently, V_C does not experience significant

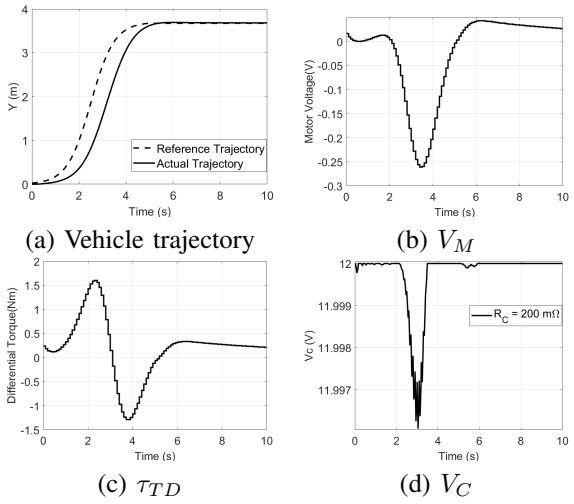

(a) Vehicle trajectory (b) V_M

(c) τ_{TD} (d) V_C

Fig. 5. Simulation results for mitigation strategy (i).

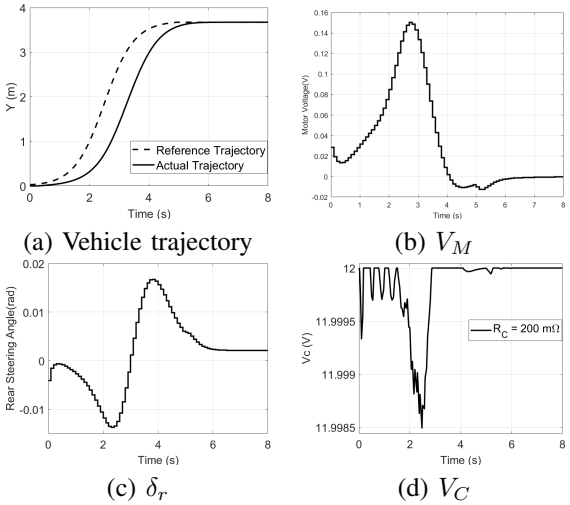

(a) Vehicle trajectory (b) V_M

(c) δ_r (d) V_C

Fig. 6. Simulation results for mitigation strategy (ii).

drops, unlike in the baseline simulation. This indicates that differential torque mitigates potential loss of steering caused by increased R_C.

Note the motor voltage and differential torque actuation take a long to converge to their nominal values. We envision that optimal selections of MPC parameters (e.g., weights in MPC cost functions) may alleviate this issue.

C. Mitigation strategy (ii) simulation

Rear steer is used with EPS for completing the desired steering maneuver. Rear steer is achieved by adjusting the angle of the rear wheels to assist in generating the required yaw moment for steering. Fig. 6 shows the resulting lane change maneuver, motor voltage (V_M), calculated rear steer angle, and the values of V_C for $R_C = 200$ mΩ. The following observations are made:

(a) Trajectory following: As with the previous simulations, the control inputs calculated by the MPC controller ensures trajectory following. The vehicle follows the reference trajectory, maintaining reasonably small lateral position y errors during the lane change maneuver. This highlights the effectiveness of MPC in managing complex dynamics, coordinating the steering redundancies.

(b) Improved EPS voltage stability: The introduction of rear steer significantly alleviates the load on the EPS motor by distributing the steering effort. Consequently, V_C does not experience a significant drop, unlike in the baseline simulation. This indicates that differential torque mitigates the potential loss of steering caused by increased R_C.

D. Mitigation strategy (iii) simulation

Both differential torque and rear steer are used with the EPS for steering. Fig. 7 shows the motor voltage (V_M), differential torque, rear steer angle, and values of V_C for $R_C = 200$ mΩ. Note that since the resulting lane change maneuver is similar to those in Strategies (i) and (ii), it is omitted here in the interest of space. The following observations are made:

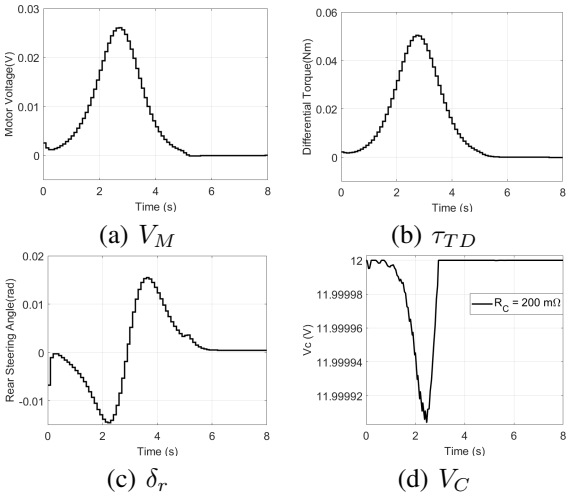

(a) V_M (b) τ_{TD}

(c) δ_r (d) V_C

Fig. 7. Simulation results for mitigation strategy (iii).

(a) Trajectory following: As with the previous simulations, the MPC controller ensures trajectory. The vehicle follows the reference trajectory, maintaining reasonable lateral position (y) errors during the lane change maneuver. This highlights the effectiveness of MPC in managing complex dynamics,

coordinating the steering redundancies.

(b) Improved EPS voltage stability: The introduction of differential torque and rear steer significantly alleviates the load on the EPS motor by distributing the steering effort. As a result, the EPS PEC voltage does not experience a significant drop.

To highlight efficacy of the fault mitigation strategies, we observe that the minimum V_C for the baseline, Strategy (i), Strategy (ii), and Strategy (iii) simulations are 10.55, 11.99, 11.99, and 11.99 Volts, respectively. The proposed strategy can effectively mitigate potential loss of steering caused by increased R_C.

VI. Conclusion and Future Work

In this paper, fault mitigation for AVs with increased resistance in EPS power circuit is considered. In particular, potential loss of steering due to decreased voltage seen at the EPS PEC and reduced electrical power transfer capability can be avoided by using MPC to coordinate redundant lateral motion actuation such as EPS, steering differential torque, and rear steering. Specifically, while the vehicle can still satisfactorily complete desired lane change maneuvers, the EPS steering effort is reduced, keeping the voltage at the EPS PEC at a high level and avoiding total steering loss. Future work include:

- experimental verifications for developed methods;
- developing methods to automatically optimize MPC cost function weights based on EPS power circuit resistance level and desired trajectories;
- developing fault mitigation strategies for multiple actuation failures and other vehicle subsystems.

References

[1] SAE On-Road Automated Driving Committee, "Taxonomy and definitions for terms related to driving automation systems for on-road motor vehicles," *SAE J3016 Standard*, 2021.

[2] M. McFarland. (2020) GM and Honda unveil self-driving car with no steering wheel or pedals. [Online]. Available: https://www.cnn.com/2020/01/22/tech/cruise-origin-gm-honda/index.html

[3] W.-C. Lin and Y. A. Ghoneim, "Model-based fault diagnosis and prognosis for electric power steering systems," in *Proceedings of the 2016 IEEE International Conference on Prognostics and Health Management*, Ottawa, Canada, 2016, pp. 1–8.

[4] A. Mohtat, G. Garner, W.-C. Lin, and N. Mehrabi, "Validation and refinement of a steering friction increase detection algorithm using test drive data," in *Proceedings of the Annual Conference of the Prognostics and Health Management Society*, 2020.

[5] W.-C. Lin and X. Du, "Prognosis of power connector disconnect and high resistance faults," in *Proc. of the 2018 IEEE International Conference on Prognostics and Health Management*, 2018.

[6] W.-C. Lin, G. Garner, Y.-C. S. Tang, and A. Mohtat, "Electric power steering power circuit health assessment and mitigation strategy," in *Proceedings of the Annual Conference of the Prognostics and Health Management Society*, 2021, pp. 1–11.

[7] N. Bomey. (2018) GM recalls 1 million pickup trucks, SUVs that could suffer steering malfunction. [Online]. Available: https://www.usatoday.com/story/money/cars/2018/09/13/gm-chevrolet-gmc-truck-recall/1289064002/

[8] Y. Jiang, H. Meng, G. Chen, C. Yang, X. Xu, L. Zhang, and H. Xu, "Differential-steering based path tracking control and energy-saving torque distribution strategy of 6wid unmanned ground vehicle," *Energy*, vol. 254, no. 1, pp. 1–15, 2023.

[9] P. Valdes-Dapena. (2021) The 2024 GMC Hummer SUV is a large 830-horsepower electric family hauler. [Online]. Available: https://www.cnn.com/2021/04/03/business/gmc-hummer-ev-suv/index.html

[10] J. Lee and H. Su, "A unified industrial large knowledge model framework in industry 4.0 and smart manufacturing," *IJAMD*, vol. 1, no. 2, pp. 41–47, 2024.

[11] H. Su and J. Lee, "Machine learning approaches for diagnostics and prognostics of industrial systems using open source data from phm data challenges: A review," *IJPHM*, vol. 15, no. 2, 2024.

[12] H. Kazemi, X. Du, S. Drame, R. Dixon, and H. Sadjadi, "Health indicators to estimate brake rotor thickness variation," in *Proceedings of the Annual Conference of the Prognostics and Health Management Society*, Scottsdale, AZ, 2019, pp. 1–6.

[13] X. Du, L. Mai, H. Kazemi, and H. Sadjadi, "Fault detection and isolation for brake rotor thickness variation," in *Proceedings of the Annual Conference of the Prognostics and Health Management Society*, Nashville, TN, 2020, pp. 1–8.

[14] H. Kazemi, X. Du, and H. Sadjadi, "A method to detect and isolate brake rotor thickness variation and corrosion," *IJPHM*, vol. 14, no. 1, pp. 1–15, 2023.

[15] A. Li, Y. Chen, X. Du, and W.-C. Lin, "Enhanced tire blowout modeling using vertical load redistribution and self-alignment torque," *ASME Letters in Dynamic Systems and Control*, vol. 1, pp. 1–6, 2021.

[16] ——, "Should a vehicle always deviate to the tire blowout side? – a new tire blowout model with toe angle effects," *Journal of Dynamic Systems, Measurement and Control*, vol. 143, 2021.

[17] A. Li, Y. Chen, W.-C. Lin, and X. Du, "A novel trust-based shared steering control for automated vehicles with tire blowout," in *Proceedings of the 2023 American Control Conference*, San Diego, CA, 2023, pp. 1129–1134.

[18] ——, "A novel IDS-based control design for tire blowout," in *Proceedings of the 2021 Modeling, Estimation, and Control Conference*, Austin, TX, 2021, pp. 179–184.

[19] Y. Huang, F. Wang, A. Li, Y. Shi, and Y. Chen, "Development and performance enhancement of an overactuated autonomous ground vehicle," *IEEE/ASME Transactions on Mechatronics*, vol. 26, no. 1, pp. 33–44, 2021.

[20] C. Yang, B. Leng, L. Xiong, and X. Yang, "Fault-tolerant path tracking control of distributed electric unmanned vehicle based on differential steering," in *2021 33rd Chinese Control and Decision Conference*, 2021, pp. 1875–1880.

[21] T. Stolte, "Actuator fault-tolerant vehicle motion control: A survey," 2021. [Online]. Available: https://arxiv.org/abs/2103.13671

[22] E. F. Camacho and C. Bordons, *Model Predictive Control*, 2nd ed. Springer, 2004.

[23] S. V. Raković and W. S. Levine, *Handbook of Model Predictive Control*. Birkhauser, 2019.

[24] A. G. Ulsoy, H. Peng, and M. Çakmakci, *Automotive control systems*. Cambridge University Press, 2012.

[25] C. Rother, Z. Zhou, and J. Chen, "Development of a four-wheel steering scale vehicle for research and education on autonomous vehicle motion control," *IEEE Robotics and Automation Letters*, vol. 8, no. 8, pp. 5015–5022, 2023.

[26] S. Huang and J. Chen, "Event-triggered model predictive control for autonomous vehicle with rear steering," in *WCX SAE World Congress Experience*, 2022, pp. 1–9.

[27] P. C. Sen, *Principles of Electric Machines and Power Electronics*, 3rd ed. Wiley, 2013.